

MEASUREMENTS OF BEAM BEHAVIOR IN THE KARLSRUHE CYCLOTRON

Helmut Dietrich  
 AEG-Forschungsinstitut  
 Frankfurt(Main), Germany

Abstract

From the measurements made during the first operation period of the Karlsruhe cyclotron those of radial beam density, phase width and axial beam distribution are mentioned. Because of the satisfactory separation of the single orbits in a large radial range it has been easy to obtain information on the energy gain per turn, the amplitudes of the coherent radial oscillation and the radial dependence of the radial and axial betatron frequencies.

Introduction

Design and construction of the Karlsruhe cyclotron have already been described in former publications<sup>1-3</sup>. This report can therefore be confined to some measurements made during the first operation period.

Radial Distances between the Orbits

Fig.1 reproduces a record of the radial beam density versus radius which was gained by means of a remote-controlled target unit running at a constant azimuthal position in the middle of a hill. The density probe had a radial extension of 0.2 mm in this case.

This record was taken after some optimizing work which concerned the position of the ion source, the amplitude of r-f voltage and the currents of the trim coils. The corrections necessary with the trim coils were in the range between 2 and 10 gauss for the isochronous field and between 3 and 9 gauss for the first harmonic. The phases indicated by the 5 phase probes fixed at the end of each trim coil range were zero.

Because of the satisfactory separation of the single orbits it has been easy to obtain some information on the beam behavior. By measuring the distances between the orbits (up to the 200th turn in this case, corresponding to about 85% of the full radius) and plotting them versus the number of turns, diagrams as that one shown in Fig.2 were obtained. Beside these measured distances 3 other curves are drawn in this figure:

To eliminate measuring errors and to exclude any possible influence of the

$\nu_r$ -oscillation on the radial distances, the arithmetic means were taken from 5 neighbors each time (curve b), and other mean values were calculated from a parabola laid through 11 neighbors according to the least squares method (curve c). From these mean-value-curves one can recognize that the beam accomplishes a coherent radial oscillation.

Without the latter the radial distances between the orbits should obey the following equation:

$$\Delta r \approx \frac{\Delta E_0 (1 + \sum a_n)^2}{m_0 \omega^2 r (1 + \gamma r^2)}$$

In this formula  $(1 + \gamma r^2)$  takes account to the radial dependence of the accelerating voltage, and  $(1 + \sum a_n)^2$  to the structure of the orbits according to the configuration of the magnetic field. The relativistic mass increase is neglected. Applying the least squares method to this equation with the 200 measured distances, the curve d of Fig.2 was calculated. By this way the energy gain per turn  $\Delta E_0$  was found to be about 195 keV for deuterons which is in good agreement with that one gained from phase measurements.

The coherent radial oscillation versus number of turns which in Fig.3 becomes already clearly visible during the first turns of the beam, was determined by taking the differences (b - d, c - d) of the curves shown in Fig.2. The radial dependence of the betatron frequency  $\nu_r$  and the amplitudes  $A_c$  of the coherent radial oscillation were calculated by means of such diagrams.

The  $\nu_r$ -values were obtained out of the number of turns between two neighboring extrema or zeros, respectively, which correspond to half a  $\nu_r$ -period. These values (taken from Fig.3) and their arithmetic means, too, are shown in Fig.4. They correspond to average values of the respective radial ranges.

The coherent radial amplitudes  $A_c$  ranging from 1 mm to 4 mm are plotted versus radius in Fig.5. They were calculated from

$$A_c \approx \frac{\Delta(\text{EXTREMA})}{2\pi(\nu_r - 1)}$$

wherein the differences  $\Delta(\text{EXTREMA})$  were also taken from Fig.3. For comparison, values of  $A_c$  are shown in the same figure which were determined by measurements with 3 dee-probes. These were made at radii nearly corresponding to the peaks and valleys of the density record (Fig.1). The radial alterations of the coherent amplitudes visible in Fig.5 are due to changes of the first harmonic of the magnetic field which were estimated to be less than 4 gauss.

#### Phase Width of the Internal Beam

One reason for the separation of the single orbits in a large radial range seems to be the design of the central region resulting in a rather narrow phase width of the beam during the first turns<sup>2</sup>. To control the further phase-development, measurements were made in Karlsruhe according to the method devised by Garren and Smith<sup>8</sup>.

For example the radial dependence of the total deuteron current at different shifts of the radio-frequency is reproduced in Fig.6. Here, heavy detuning of the resonance condition is accompanied by an increase or loss of ion current in the central part of the cyclotron. As the operational conditions of the ion source remained constant during these measurements, the alterations of the ion current seem to be due to the slits programming the first orbits and possibly to a small failure of the magnetic field in this region.

All phase values shown in the next figures were calculated with an expanded Garren-Smith-formula

$$\sin \phi(\tau_0) \approx \pm 1 - \frac{4r^3 m_0 f \Delta f}{3 \Delta E_0} \left( \tau_0^2 + \frac{1}{2} \gamma \tau_0^4 \right)$$

where the term  $\frac{1}{2} \gamma \tau_0^4$  takes account to the radial dependence of the accelerating voltage<sup>7</sup>, whereas the influence of the relativistic mass increase is neglected.

From the distributions of Fig.6 the phase band of the deuteron current as shown in Fig.7 was derived. Here one can recognize that the steps of the records in the medium radial range indicate a small oscillation of the phase band and that the increase or loss of total current in the central part as mentioned above is accompanied by some broadening or narrowing of the phase band in this region.

Taking intervals of 10% of the total currents at the slopes, where the beam is detuned for  $\pm 90$  degrees with reference to radio-frequency, one receives

the radial dependence of the phase-subbands, which are shown for positive frequency shifts in Fig.8. The apparent spread of these subbands in the radial range between 50 cm and 65 cm is due to the fact that the phase band is oscillating and the frequency shifts were too rough.

At a radius  $r_0 = 38$  cm, where the inclination of the subbands is nearly the same, the phase profile of the beam was determined from the values shown in Fig.8. The result is given in Fig.9: the total phase width amounts to  $(20 \pm 5)$  degrees with reference to radio-frequency, and about 50% of the ion current are conducted within a phase interval of approximately 7 degrees.

A further example of phase measurements is shown in Fig.10, which were carried out with alphas. In this case the resonance condition was only roughly fulfilled by changing the radio-frequency and the main magnetic field with reference to the operational conditions with deuterons, whereas the trim coil system remained unchanged. The frequency shifts applied were in the range between + 90 kHz and - 30 kHz at a resonance frequency of 33.080 MHz. The phase width derived from these measurements amounts to some 30 degrees. The increase in comparison with the value obtained with deuterons seems to be due to another type of the ion source (geometry of the slot) and its position.

No hint for a remarkable phase compression versus radius was found with alphas and deuterons, too. The energy gain per turn  $\Delta E_0$  resulting in a covering of the phase bands for positive and negative frequency shifts was found to be about 200 keV for deuterons and 400 keV for alphas. The corresponding values from the beam density records taken at the same run were  $(198 \pm 6)$  keV and  $(408 \pm 10)$  keV respectively.

#### Axial Beam Distribution

Some measurements were made with a 3-finger probe by using the remote-controlled target unit mentioned above. The ion currents on the single fingers were registered with the same cyclotron adjustment as used for the beam density record shown in Fig.1. They were recorded one after another and controlled as to reproducibility. An example of these measurements is given in Fig.11. One can recognize that approximately 70 to 80% of the total ion current were striking the middle finger having an axial extension of 3 mm and that the beam is performing a coherent axial oscillation,

too. The latter was amplified by a poor adjustment of the ion source for about 1 mm in its axial position.

By measuring the radii of the beam density peaks on the upper or lower finger respectively and assigning to these radii the interpolated numbers of turns which were obtained from the radial density measurements (Fig.1), it is possible to calculate the axial betatron frequency  $\nu_z$  in the radial range wherein the single turns are separated enough for measurements of their radii. The result of this calculation is given in Fig.4. The  $\nu_z$ -values plotted there are the arithmetic means of 3 neighboring values derived directly from the records shown in Fig.1 and Fig.11.

The small oscillations of the radial and axial betatron frequencies as shown in Fig.4 cannot be due to the alterations of the magnetic field index  $k$  induced by the trim coils. Having the same radial periodicity they are to be explained by the shape of the pole sectors. Steps in these sectors are combined with minima of the axial betatron frequency  $\nu_z$  and maxima of the radial betatron frequency  $\nu_r$ , whereas the regions with larger distances between two steps produce a reversed effect because of the magnetic field index  $k$  being smaller than the demanded theoretical value.

Another measurement of the axial distribution was performed by means of a 5-finger density probe as shown in Fig.12. From this record the coherent axial oscillation of the beam is clearly to be seen. It was not possible to determine the axial beam profile with better resolving power - as was aimed at - with this 5-finger density probe because of the fact that the main part

of the beam was striking only two fingers of the probe at the same turn. The axial displacement of the beam as a whole to be seen in Fig.12 was possibly caused by poor adjustment of the target unit in this case.

#### Acknowledgement

The phase measurements used for the calculations mentioned were performed together with H.H. Feldmann (AEG), E. Hartwig (AEG) and G. Haushahn (GfK). I wish to thank them and the cyclotron teams of the Gesellschaft für Kernforschung, Karlsruhe, and of the Allgemeine Elektrizitäts-Gesellschaft for their assistance, especially H. Thimmel (AEG) for his help in the numerical calculations.

#### References

1. K. Steimel and A. Lerbs, Atomwirtschaft 4 (1959), 345.
2. M. Reiser, Nucl. Instr. and Meth. 13 (1961), 55.
3. A. Kuellmer, Kerntechnik 4 (1962), 234.
4. A. Kuellmer, Vakuumtechnik 12 (1963), 37.
5. K. Steimel, CERN-report 1963-19, 24.
6. W. Wolff, AEG-HE/FI/5-F, internal report (1965).
7. H.H. Feldmann, thesis, Technische Universität Berlin (1964).
8. A.A. Garren and L. Smith, CERN-report 1963-19, 18.

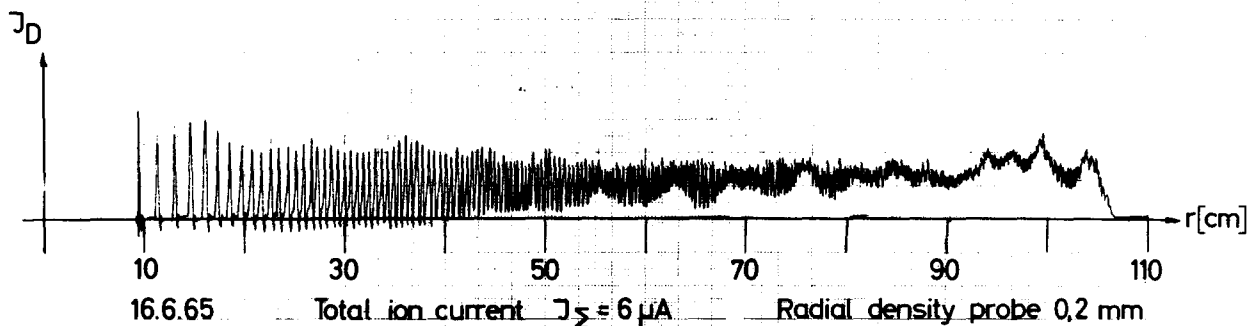


Fig.1 Beam density vs. radius

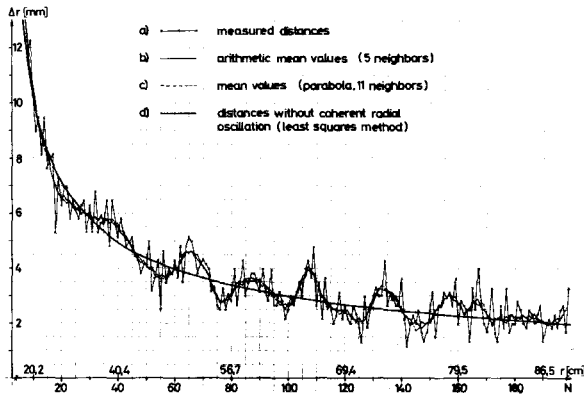


Fig. 2 Radial distances between the orbits vs. number of turns

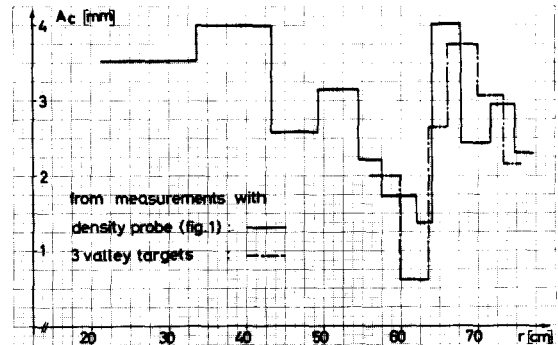


Fig. 5 Coherent radial amplitudes vs. radius

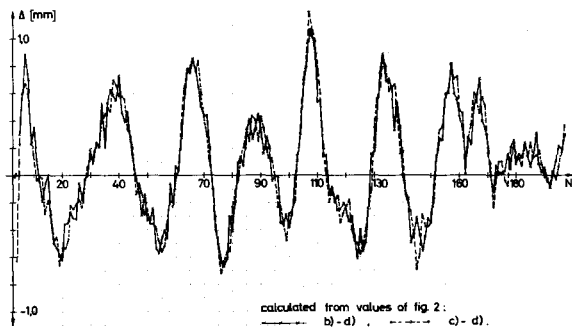


Fig. 3 Coherent radial oscillation vs. number of turns

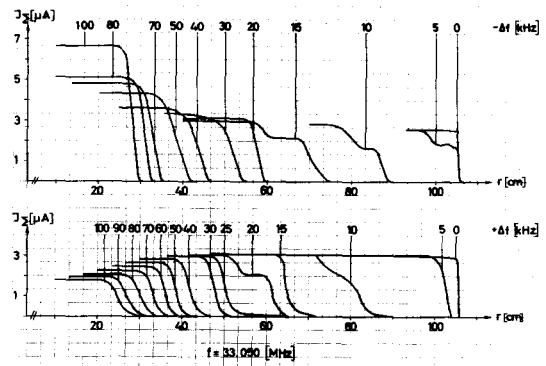


Fig. 6 Deuteron current vs. radius for different frequency shifts

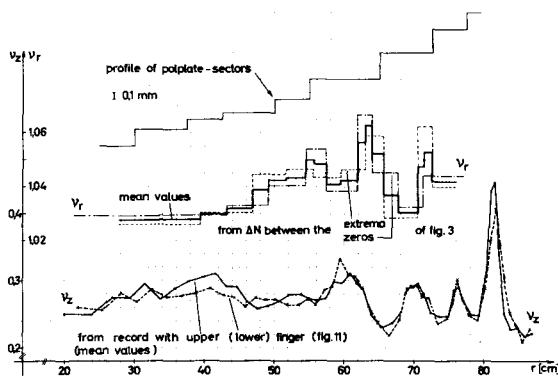


Fig. 4 Radial dependence of betatron frequencies  $\nu_r$ ,  $\nu_z$

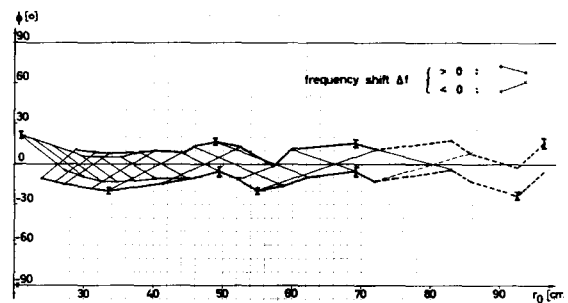


Fig. 7 Phase width of a 50 MeV d beam vs. radius

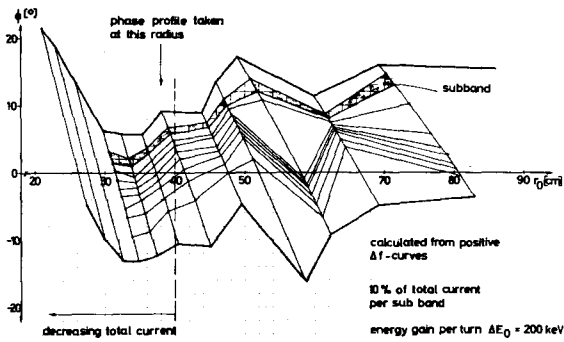


Fig. 8 Phase distribution of a deuteron beam vs. radius

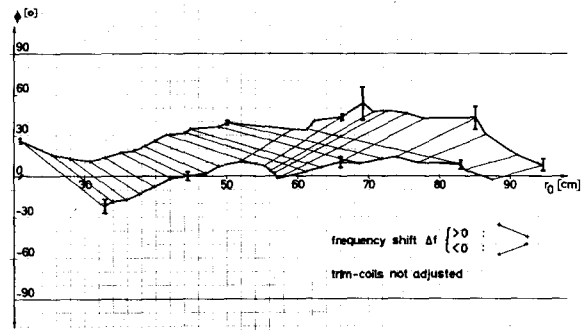


Fig. 10 Phase width of a 100 MeV α beam vs. radius

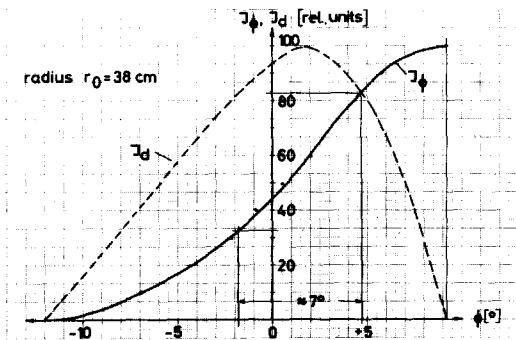


Fig. 9 Phase profile of a deuteron beam at  $r_0 = 38$  cm

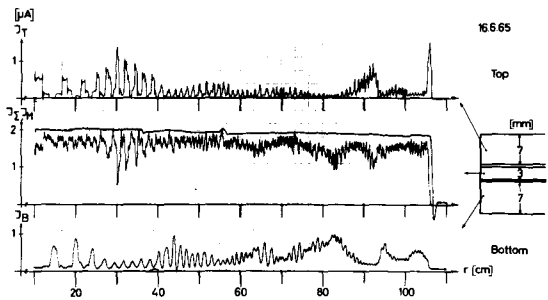


Fig. 11 Axial beam distribution measured with a 3-finger probe

DISCUSSION

HAASE: I can extend the figure for phase width which Dr. Dietrich just gave. In a time-of-flight experiment with the external beam we have recently measured the width of the particle burst and found it to be less than 0.2 nsec. This is less than 3° with respect to the rf and 1° with respect to the orbit.

BLASER: How was this done? Is it difficult?

HAASE: We shot the external beam onto a thick copper target and measured the time-of-flight spectrum with a photomultiplier and plastic scintillator.

BLOSSER: Is it possible that the bending mechanism, or other hardware of the external beam, is functioning as a bunching system?

HAASE: This was done in the direct beam. We had only a small magnet bending the beam possibly 5 or 6° and one quadrupole, no slits. The measurement was made 17 meters away from the cyclotron. The width depended somewhat on the tuning of the machine. We could also get two bursts separated by 0.3 seconds, or so, and we could suppress one or the other of the bursts. The spacing of these bursts was independent of the machine parameters, as far as we could tell, so this would speak against your argument. Also, we made measurements at 12 and 22 meters from the cyclotron, and found no evidence for bunching.

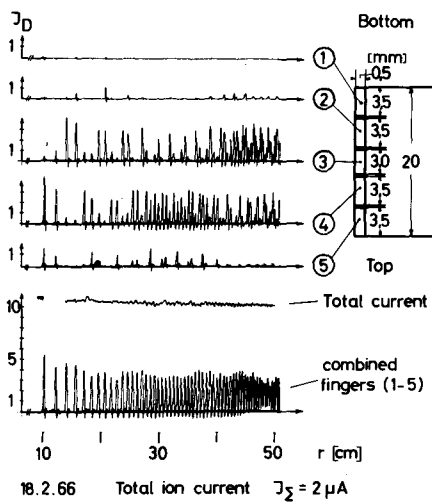


Fig. 12 Record with a 5 finger density probe